A gas ejector for CO_2 supercritical cycles

Michal Palacz[a,*], Michal Haida[a], Jacek Smolka[a], Marcin Plis[a], Andrzej J. Nowak[a], Krzysztof Banasiak[b]

[a] *Institute of Thermal Technology, Silesian University of Technology, Konarskiego 22, 44-100 Gliwice, Poland*
[b] *SINTEF Energy, Kolbjørn Hejes v. 1D, Trondheim, 7465, Norway*

Abstract

The CO_2 ejectors are recently often used as the main expansion device in the modern refrigeration cycles. On the other hand, according to the newest literature the implementation the ejectors into supercritical CO_2 power cycles increase its performance. The recent studies showed that in case of the power cycles the ejector pressure lift and mass entrainment ratio are relatively high. Therefore, the main scope of this paper is the investigation of the possibilities of designing the ejector for supercritical Brayton CO_2 system. The CFD based computational tool was used to design the ejector for the considered cycle. The system analysis was used to define the ejector on design point. The results of that analysis showed that the required pressure lift and must be equal to 103 bar and mass entrainment ratio equal to 0.995, respectively. The CFD-based evaluation of the proposed ejector showed that these values are impossible to achieve. Therefore, the modifications of the crucial ejector dimensions was performed to increase its performance. Nevertheless, the maximum possible pressure lift for the proposed ejector was equal to 60 bar The analysis of the gathered results showed that the design of the ejector fulfilling the system requirements may be impossible to achieve.

Keywords: R744 Ejector, Supercritical CO_2, CO_2 Brayton cycle, thermal performance

Nomenclature

D	diameter, m
E	total enthalpy, J kg^{-1}
h	specific enthalpy, J kg^{-1}
k	effective thermal conductivity, W m^{-1} K^{-1}
L	length, m
$\dot{m}$	mass flow rate, kg s^{-1}
N	net power, W
p	pressure, Pa
$\dot{Q}$	heat transfer rate, W
r	pressure ratio, -
T	temperature, °C
t	time, s
s	specific entropy, J kg^{-1} K^{-1}
U	velocity vector, m s^{-1}

Greek letters

χ	mass entrainment ratio, -
η	efficiency, -
ϵ	heat loss factor, -
γ	angle, °

*Tel.: +48 322372810; fax: +48 322372872
michal.palacz@polsl.pl

This is the accepted version of an article published in Energy.
DOI: 10.1016/j.energy.2018.09.030

ρ density, kg m^{-3}

τ stress tensor, N m^{-1}

Subscripts

C compressor

heat heater

high highest parameter in the system

HX heat exchanger

MN motive nozzle

SN suction nozzle

T turbine

1. Introduction

The latest regulations of the European Union on the fluoride greenhouse gases (so-called F-gas regulation) [1] effectively limit the usage of the numerous working fluids. According to that regulation, the high Global Warming Potential (GWP) fluids should be withdraw from the market until 2020 [2]. Due to those legislation issues and the excellent thermodynamic properties, carbon dioxide [3, 4] is more often utilised as a working fluid. This CO_2 revival is especially noticeable in the modern refrigeration industry [5]. As the authors of [6, 7] presented, the most advanced commercial units installed in the European Union and in the United States of America are CO_2-based systems. Moreover, the current literature data shows that carbon dioxide is suitable for both power generation and co-generation systems. Kim *et al.* [8] showed that depending on the heat source, such systems can operate in a transcritical or supercritical mode. For systems with high- temperature heat sources, such as thermal solar plants or nuclear power plants, the supercritical CO_2 (sCO_2) Brayton cycle offers a reasonable increase in the system performance [9]. The literature [10] shows that the thermal efficiency of a well-designed sCO2 Brayton cycle can exceed an efficiency of 40%. It is also worth noting that there are various Brayton cycle systems studies presented in the literature. A comparison of the numerous system layouts has been performed in [11]. The authors of this investigation illustrate how the thermal efficiency of the system increases with the system's complexity. According to the results presented by the authors, the most efficient solution is the recompression cycle with heat recovery and intercooling. In this configuration, the thermal efficiency of the system was higher than 50%. In addition, the size of the heat exchanger for such a setup is smaller than for the equivalent set up without an intercooler. More comprehensive analysis of the sCO_2 Brayton cycle was conducted in [12]. The authors investigated a similar range of the Brayton cycle designs given in [11], and [12] showed that implementation of an ejector into the sCO_2 system is beneficial. The introduction of the ejector into such a system configuration reduces the pressure at the solar receiver. Moreover, the thermal efficiency of the ejector aided the system is similar or even higher than a classical cycle. Conversely, the authors of [12] present an optimal turbine split ratio that requires the ejector's mass entrainment ratio to be equal to ~1.0 for pressure lift equal up to 100 bar. For refrigeration carbon dioxide ejectors, these parameters typically give significantly lower values. Two-phase CO_2 refrigeration systems are usually designed for a pressure lift range from 2 to 16 bar. Moreover, the mass entrainment ratio for these ejectors typically does not exceed 0.5. It is also worth noting, that in case of the single-phase ejector proposed by Padilla *et al.* [12], relatively simple 1D models were used to analyse this device's performance. The mathematical models used in [12] were originally formulated for steam ejectors published in the papers [13, 14]. Moreover, Padilla *et al.* [12] used the experimental data from R141b to validate their utilised model. In addition, in this model, the efficiencies of different ejector sections were taken from the literature values from steam ejectors [15]. Hence, a more detailed investigation of the CO_2 ejector designed for such a system is desired to confirm the performance of the single-phase ejector in the proposed power system.

This is the accepted version of an article published in Energy.
DOI: 10.1016/j.energy.2018.09.030

As previously noted, the authors of [12] use a relatively simple mathematical model (formulated specifically for steam ejectors) to simulate their ejector work, this is a common approach used to investigate the ejector performance. Various mathematical models have also been developed specifically for the CO_2 ejectors. The most popular and one of the simplest models used for analysis of a two-phase refrigeration ejector is given in [16]. In this approach, the 1D mathematical model was divided into the sub-models for each part of the device, meaning the global parameters describing the ejector performance can be obtained. A similar approach was used by Liu *et al.* [17], where the models of the specific ejector sections were coupled to calculate the devices performance. Moreover, similar to [12] the isentropic efficiencies of each ejector part were arbitrarily defined. Banasiak and Hafner [18] also used a 1D model for the carbon dioxide ejector design and simulation. However, the authors of this model investigated the influence of a two-phase flow model on the accuracy of the formulation [19]. To better understand and illustrate the fluid flow inside the device, more complex and advanced mathematical models are needed to be applied, such as CFD based models. The authors of [20] proposed CFD models with a homogeneous equilibrium model (HEM), which is implemented for two-phase flow simulations. Authors of [19] and [20] validated the models for operating conditions typical for a CO_2 based heat pump system. In addition, the authors of [20] validated the model for the gas ejector for R141b. In [21] the authors investigated the limitations and application range of the HEM (used both in [20] and [22]) for the simulation of the carbon dioxide flow inside the two-phase flow ejectors. The research shows that HEM guarantees the acceptable accuracy for motive nozzle operating regimes close to or above the critical point of the carbon dioxide. Moreover, the same authors performed an analysis and comparison of the accuracy of the equilibrium and relaxation models for two-phase flow presented in [23]. According to their results, the homogeneous equilibrium model offers a higher fidelity than the homogeneous relaxation model (HRM) for operating regimes distributed above the critical point of the fluid. The influence of the relaxation time on the HRM fidelity is presented in [24]. The authors of [24] optimised the relaxation time for various motive nozzle operating conditions to guarantee the high fidelity of the model. Nevertheless, the ejectors employed in sCO_2 systems operate only in single-phase region. Therefore, the two-phase flow models were not in use in case of the simulation presented in this paper. On the other hand, despite the modelling approach used, the CFD models are still relatively computationally time expensive. Therefore, the numerous authors proposed different modelling approaches for the ejector performance analysis. Besagni *et al.* [25] proposed the lumped parameter model for an assessment of the ejector performance. That model was developed for on- and off-design condition of fixed geometry ejector. Moreover, the authors of aforementioned approach used the CFD model of the ejector in order to map the ejector sections efficiencies and then implement these maps into the lumped parameter model. It should be pointed out that the authors of [25] used an ideal gas for the fluid properties modelling. In consequence, the comprehensive validation procedure presented in that paper was mostly focused on comparison of the experimental and CFD results for the air-air ejectors. The other type of the CFD model simplification was presented in the paper [26]. The authors of that approach used both experimental and CFD results for the formulation of the hybrid reduced order model for the CO_2 ejectors for refrigeration systems. Haida *et al.* [26] used already mentioned CFD model based on the real fluid approach developed by Smolka *et al.* [20] for CO_2 ejector enhanced with the HRM for the two-phase flow. Nevertheless, that reduced order model is useful only for the already known ejector geometry. Therefore, it is suitable for dynamic system modelling for a priory known ejector shape and performance for the various operating conditions used for the reduced order model preparation. The mentioned above simplification of the CFD models are very useful for fast computations for the ejector performance evaluation. However to design high efficient ejector, the information about the local and field values of the

This is the accepted version of an article published in Energy.
DOI: 10.1016/j.energy.2018.09.030

fluid flow are desired. Thus, the authors of this study utilised the CFD model presented in [20] for the ejector design procedure.

The mathematical model presented by [20] was also used for two-phase ejector shape optimisation and performance analysis ([27, 28]), and then the HRM enhanced version [23, 24] was used for reduced order model formulation [26]. The same authors implemented the developed CFD models into a computational platform for CO_2 ejector simulation, which is called *ejectorPL*. That computational tool guarantees full automation of the simulation process and reduces the computational time. In [29], the *ejectorPL*, combined with optimisation algorithms, was used to optimise the shape of the carbon dioxide ejectors for the refrigeration systems. The optimised ejector shapes offered an efficiency equal to or higher than 30% over a given range of operating conditions. Therefore, the combination of *ejectorPL* and optimisation procedures can be considered as the most efficient and robust computational tool for ejector design.

To the best of our knowledge, the application of the CFD tools to a sCO_2 ejectors analysis has not been published. Hence, the scope of this paper is to investigate the ejector design that fulfils the performance requirement presented in [12]. In particular, the possibility of the ejector design that achieve the mass entrainment ratio equal to ~1 for pressure lift that exceeds 100 bar. Consequently, two ejector designs were proposed to fulfil the ejector requirements defined in the paper of Padilla *et al.* [12]. The mentioned authors adopted idea of introducing the ejector into the system from the study presented in [30]. They also suggested that the investigated ejector equipped cycle can be integrated with Concentrated Solar Thermal system. Moreover, Padilla *et al.* [12] investigated numerous system configurations e.g. recompression cycle or multi-recompression cycle. Nevertheless, the analysis in [12] was mostly theoretical. Therefore the presented approach can be integrated, both direct or indirect, into various sCO_2 based systems. In consequence, the authors of this study decided to investigate the simplest of system layout analysed in [12] was considered in this study. influence of the pressure lift and mass entrainment ratio for each design was investigated. The collected results show the maximum ejector mass entrainment ratio that was possible to achieve a desired pressure lift. Consequently, the limitations of the ejector design for the sCO_2 Brayton cycle are given.

2. Supercritical CO_2 systems

Supercritical CO_2 cycles offer a large potential for thermal efficiency, when high temperature heat sources are available. According recent studies presented i.e. [8] the sCO_2 Brayton are suitable for high-grade heat sources. Thus, the significant effort of the research community was invested to investigate the possibility of the integration CO_2 Brayton cycle with i.e. nuclear power plants or solar thermal power plants. Garg *et al.* [31] showed the possibility of the integration of the CO_2 Brayton cycle to solar power application. Moreover, the authors of that research suggested that in case of the supercritical operation the Brayton cycle is more efficient comparing to e.g. transcritical systems. In addition, the authors of [9] discussed numerous variants for the integration of the sCO_2 Brayton cycles. In that paper the benefits of the application of the ejector into CO_2 are briefly discussed. In particular, the authors of that study summarised the recent development of the sCO_2 systems. The integration of the supercritical Brayton cycle with the solar thermal power plant has been investigated in [32]. The authors of that research compare the direct and indirect integration of a solar tower loop with the Brayton cycle. The indirect set up is presented in Fig. 1, showing that the Brayton cycle is indirectly integrated with the solar tower loop. In the work presented in [32], the advantages and disadvantages of both solutions are given. In addition to the various methods for the implementation of sCO_2 with heat sources, a large number of Brayton cycle configurations are also possible [33]. It should be noted that in literature are presented different

This is the accepted version of an article published in Energy.
DOI: 10.1016/j.energy.2018.09.030

approaches sCO_2 Brayton integration within the power system. Namely, the direct integration of the supercritical carbon dioxide Brayton cycle and power system such as presented in [34]. Nevertheless, the integration approach is out of the scope of this study. Therefore, the influence of the integration set up on the system performance was not investigated through this study.

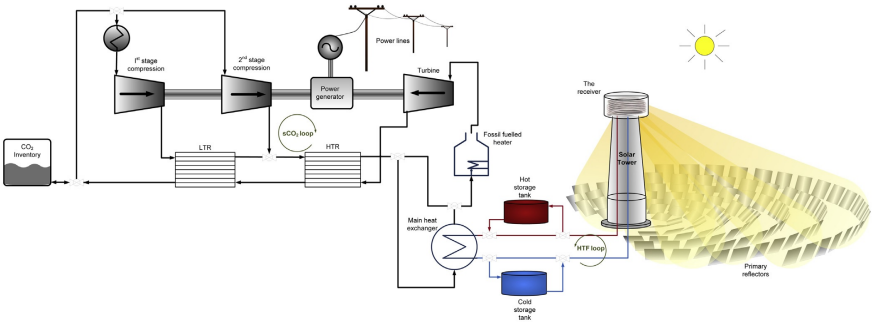

Figure 1: Indirect integration of the solar thermal plant with the Brayton cycle ([32])

Padilla *et al.* [12] demonstrated the possibility of the implementation of an ejector into almost any Brayton cycle configuration, the introduction of this device into the system results in a performance increase. Comparison of a classical sCO_2 Brayton and an ejector equipped system is presented in Fig. 2. A relatively simple cycle with one recuperator for heat recovery and an intercooler is presented. In case of the ejector system, the stream that leaves the heater is divided into the two streams. The first stream is directly expanded into Turbine 1 (T1) and then flows through the recuperator and cooler to the compressor. Next the fluid, via the recuperator, is heated and sent to the ejector motive nozzle. Inside the motive nozzle the stream is expanded to give a pressure significantly lower than the Turbine 2 (T2) outlet pressure. The second part of the carbon dioxide leaving the heater is expanded into Turbine 2. Next the fluid travels to the ejector suction nozzle. Finally, both streams are mixed inside the mixing section of the ejector. In this part of the device, momentum transfer between the streams occurs. Inside the ejector diffuser the velocity of the fluid decreases and the pressure of the fluid increases. Thus, the pressure of the fluid is notably higher than at the Turbine 2 outlet. The system optimisation results presented in [12], show that the turbine mass flow rate split ratio should be equal to 0.5 the pressure lift equal 102 bar. Consequently, the mass entrainment ratio of the ejector installed into this cycle should be equal to ~1. For the configuration discussed by the authors in [12], a similar or slightly higher efficiency of the system is observed, when comparing the system layout without an ejector. Moreover, for the sCO_2 system equipped with the ejector, the heater pressure was also reduced resulting in the improved durability and thermodynamic performance of that heat exchanger.

3. Mathematical modelling

In this section, the details of the mathematical model employed for the computations used are discussed. Both, system modelling and ejector modelling were conducted under steady state conditions. The CFD simulations were performed on the Institute of Thermal Technology (ITT) computational cluster, named TOLA. This unit consists of 13 computing nodes, each equipped with two Intel Xeon processors (10 physical cores per processor). Therefore, TOLA offers 260 cores for parallel computations. For the system simulations, the F-Chart Engineering Equation Solver was executed on a standard desktop computer.

This is the accepted version of an article published in Energy.
DOI: 10.1016/j.energy.2018.09.030

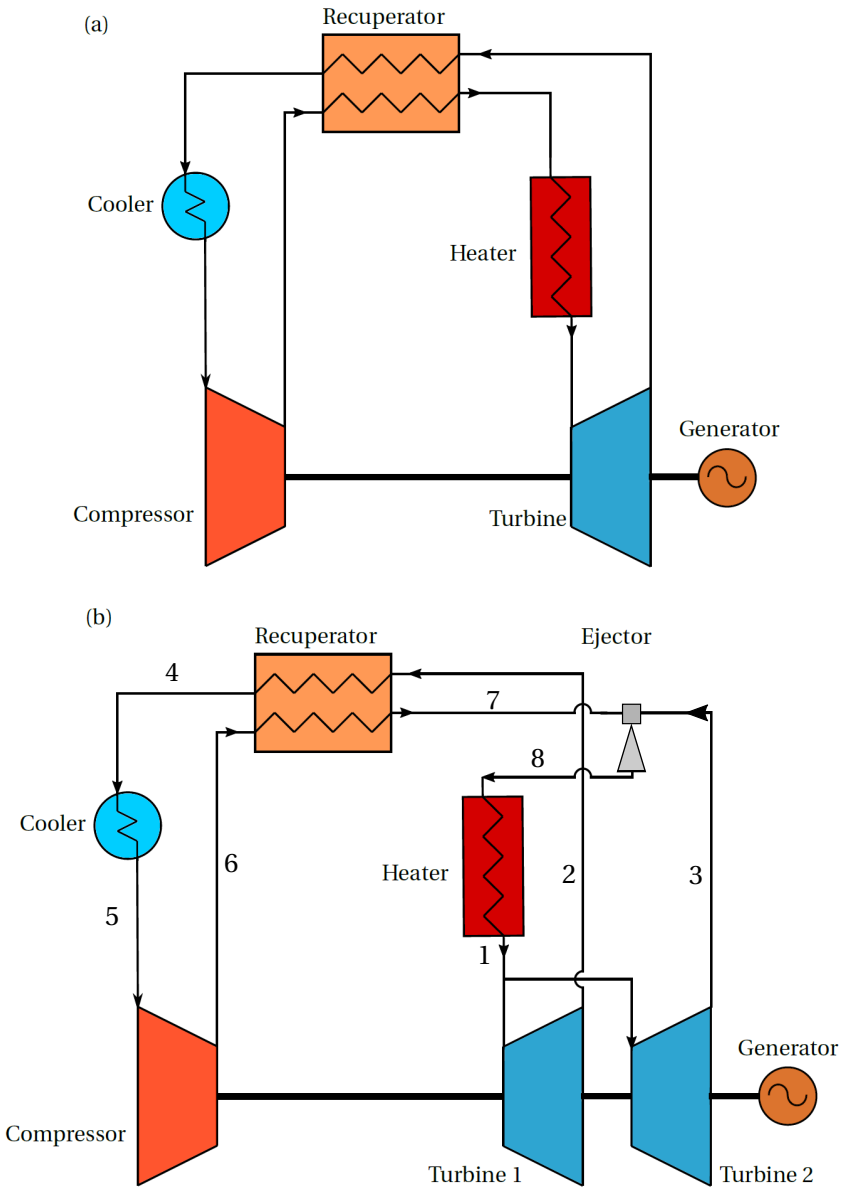

Figure 2: Comparison of the Brayton cycle without (a) and with ejector (b), adapted from [12]

This is the accepted version of an article published in Energy.
DOI: 10.1016/j.energy.2018.09.030

3.1. Ejector modelling

A baseline ejector design was obtained by the utilisation of the 1D model introduced in [19]. That model was previously used to design ejectors for a novel multi-ejector refrigeration system [35]. Within this relatively simple yet robust model, the motive nozzle was carefully designed. Next, the mixing section was designed. The shape of that ejector part was defined with cross- section area ratios of the motive nozzle throat and mixer diameter and length similar to that proposed for refrigeration ejectors ([35]). Nevertheless, as shown in [29], the addition of CFD modelling into the ejector design procedure is a possible way to achieve high performance ejectors.

The CFD tool, named *ejectorPL*, was used for the ejector design and performance analysis. This computational script is a combination of the pre-processor (Ansys ICEMCFD), solver (Ansys Fluent) and in-house developed post processing procedures. The mathematical model implemented in this tool is based on the model developed by [20]. It is worth noting, that the considered mathematical model was validated for both two-phase and single-phase gas ejectors. Nevertheless, the original [20] model was enhanced by 2D axisymmetric computation capability and optional computations with the homogeneous equilibrium or advanced relaxation model (HEM or HRM) for two-phase flow [20, 23, 24]. The reduction in the computational domain for the 2D case reduces the computational time notably. For all simulated cases a numerical grid was fully structural. The meshes used for the ejector design consisted of approximately 35k elements. Then, for the performance analysis of the final ejector design the computational mesh was refined up to 135k cells. The coarse and refined meshes are presented in Fig. 3. As

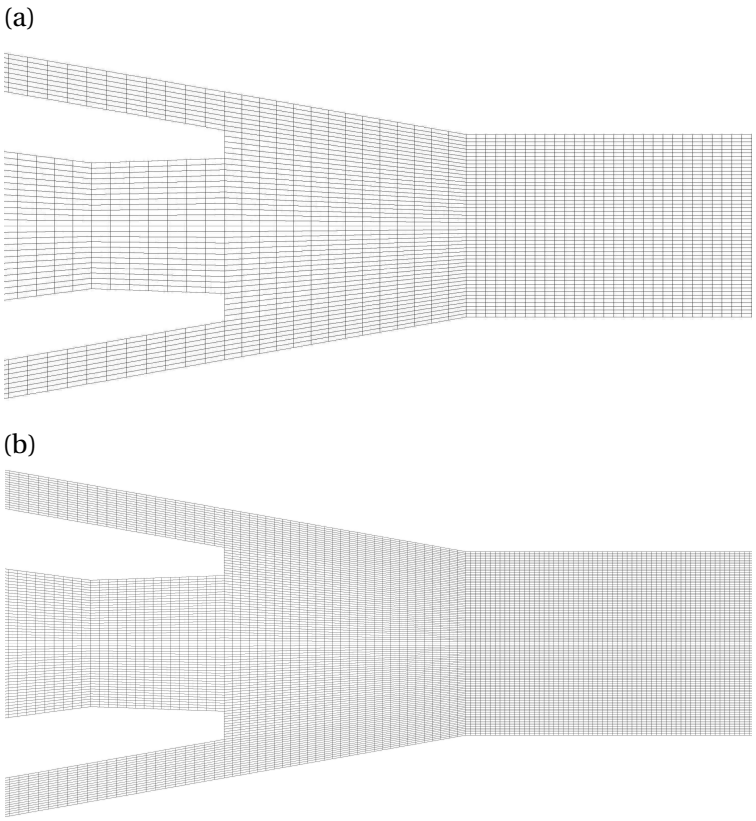

Figure 3: Numerical domains, (a) coarse mesh and (b) refined mesh

This is the accepted version of an article published in Energy.
DOI: 10.1016/j.energy.2018.09.030

observed, the number of elements was significantly higher in the nozzle and pre-mixing sections of the ejector. Moreover, the ratio between the longer and the shorter edge of the mesh element was approximately constant throughout the whole computational domain. The mesh refinement slightly influences the shape of the contours of the fluid flow. On the other hand, an increase in the number of the mesh elements inside the motive nozzle does not affect the simulated motive nozzle mass flow rate significantly. Moreover, the scope of this paper is mostly focused on the relatively fast ejector simulation for its performance assessment. Therefore, the mesh was not refined near the ejector walls for the boundary layer modelling. Such approach was also used in the previous works of the authors and guaranteed the acceptable accuracy of the ejector performance prediction, i.e. [23].

The *ejectorPL* computational tool that was employed for the simulation of the fluid flow inside the device offers the HEM and HRM two-phase flow simulations. Nevertheless, the CO_2 ejector considered in this study operates only in supercritical mode. Therefore, the two-phase flow models implemented in mentioned computational tool were not executed during the computations. Thus, to simulate the fluid flow inside the device, the following set of equations were solved:

$$\frac{\partial \rho}{\partial t} + \nabla \cdot (\rho U) = 0 \tag{1}$$

$$\frac{\partial (\rho UU)}{\partial t} + \nabla \cdot (\rho UU) = -\nabla p + \nabla \cdot \tau \tag{2}$$

$$\frac{\partial (\rho UE)}{\partial t} = \nabla \cdot (k \nabla T + \tau \cdot U) \tag{3}$$

where E is equal to:

$$E = h + \frac{U^2}{2} \tag{4}$$

According to the recent studies presented in [36] the various two equations models for the turbulence provided different fidelity of the mass entrainment ratio prediction for single-phase ejector. On the other hand, the discrepancies between the experimental and computational data for investigated turbulence models was lower than 10% which can be considered satisfying. One of these models, namely realisable $k-\epsilon$ [37, 38] was used by the authors in numerous CO_2 ejector analysis. Thus, regarding the computational time, solution strategies and convergence of the CFD model the realisable $k-\epsilon$ model was used to simulate the turbulent flow inside the device. For the real fluid properties, NIST REFPROP libraries were implemented ([39]). The detailed description of this approach is presented [20]. Moreover, the extended validation of that formulation is presented in [23].That model was also reduced to decrease the computational time and was used for ejector performance mapping [40].

The goal of CFD modelling of the device was to design an ejector that would guarantee a mass entrainment ratio equal to ~1, at a desired pressure lift and for specified inlet conditions obtained from the cycle analysis. The mass entrainment ratio is defined as:

$$\chi = \frac{\dot{m}_{SN}}{\dot{m}_{MN}} = \frac{\dot{m}_{T2}}{\dot{m}_{T1}} \tag{5}$$

Where the subscripts SN and MN stand for suction nozzle and motive nozzle. The suction nozzle mass flow rate corresponds to Turbine 2, while the motive nozzle mass flow rate is related to the Turbine 1. The typical ejector assembly can be described by 14 geometrical parameters. A simplified scheme of the ejector and its parameters are presented in Fig. 4. These parameters define the motive and suction nozzle geometry, as well as the mixing section and the diffuser shape. Nevertheless, according to the

This is the accepted version of an article published in Energy.
DOI: 10.1016/j.energy.2018.09.030

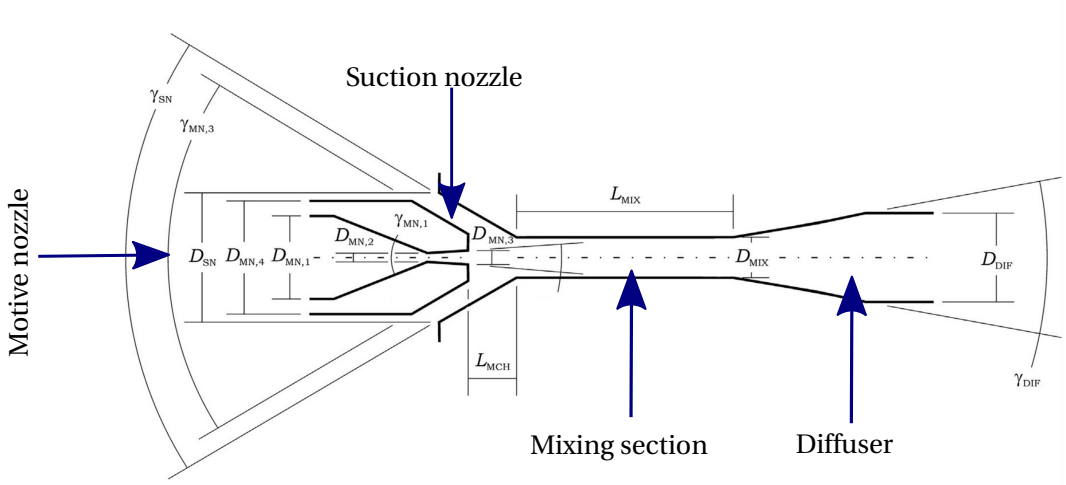

Figure 4: Typical ejector assembly (a) and geometrical parameters describing the device shape (b)

results presented in [27, 41], the mixing section design mostly affects the ejector performance. Therefore, the ejector design procedure was used to propose the initial ejector shape, for the considered sCO_2 system including two main steps. As previously noted, the motive nozzle was designed, then, the mixing section and diffuser design was proposed based on the motive nozzle throat diameter to mixing section diameter ratios, defined for the refrigeration two-phase ejectors [42]. Next, the initial ejector design was modified to investigate the influence of the parameters such as: the mixer diameter (D_{MIX}), mixer length (L_{MIX}), premixing chamber length (L_{MCH}), motive nozzle outlet diameter ($D_{MN,out}$) and the motive nozzle diverging angle (γ_{MN}).

3.2. sCO_2 Brayton cycle modelling

A supercritical CO_2 Brayton cycle layout was proposed by Padilla *et al.* [12] and it is presented in Fig. 2(b). The input parameters for the system modelling are similar to those used in [12, 43]. The list of these parameters is presented in Tab. 1. In addition, the temperature-entropy and pressure-enthalpy diagrams for the cycle input parameters listed in Tab. 1 are presented in Fig. 5. The cycle points numbering corresponds to the numbering of the characteristic points of the considered layout presented in Fig. 2(b). The subscripts MN, SN and OUT in Fig. 5 denoted motive nozzle, suction nozzle and ejector outlet, respectively. To model the cycle, the set of the equations presented bellow was defined. The heater performance was calculated using the following equation:

$$\dot{Q}_{heat} = (\dot{m}_{T1} + \dot{m}_{T2}) \cdot (h_1 - h_8) \tag{6}$$

The turbines and compressor thermodynamic relations were computed with the equations listed below:

$$\eta_{T_1} = \frac{h_1 - h_2}{h_1 - h_{2s}} \tag{7}$$

$$\eta_{T_2} = \frac{h_1 - h_3}{h_1 - h_{3s}} \tag{8}$$

$$N_{i,T1} = \dot{m}_{T1} \cdot (h_1 - h_2) \tag{9}$$

$$N_{i,T2} = \dot{m}_{T2} \cdot (h_1 - h_3) \tag{10}$$

This is the accepted version of an article published in Energy.
DOI: 10.1016/j.energy.2018.09.030

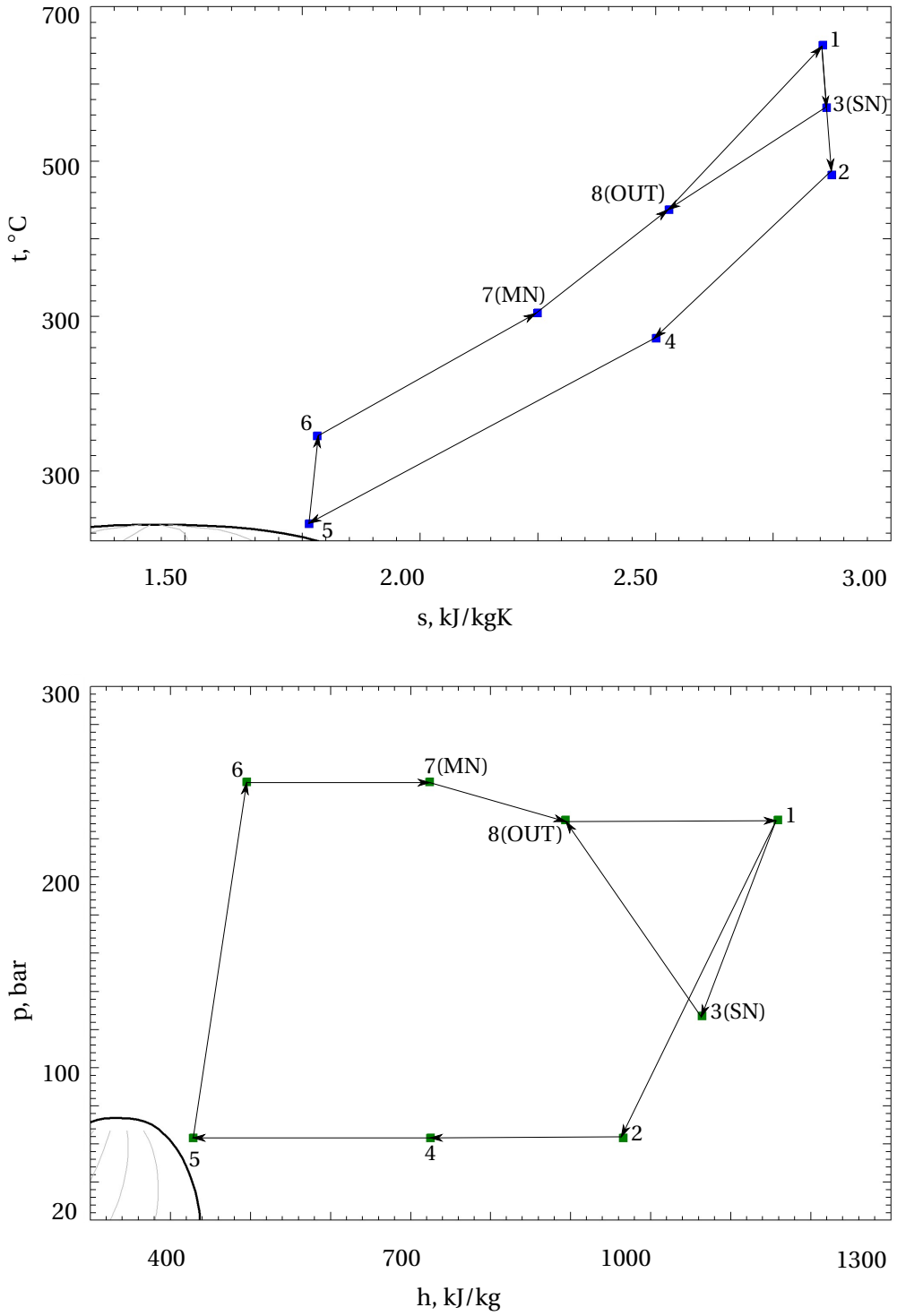

Figure 5: Temperature-entropy (a) and pressure-enthalpy (b) diagrams for the considered cycle

This is the accepted version of an article published in Energy.
DOI: 10.1016/j.energy.2018.09.030

Table 1: System modelling input parameters [12, 43]

Parameter	Value	Unit
η_T	0.93	-
η_C	0.89	-
ϵ_{HX}	0.05	-
T_1	650.00	°C
T_5	32.00	°C
$\min\Delta T_{pinch}$	5.0	K
p_{high}	250.00	bar
Δp_{red}	0.08	-
r_{T1}	3.65	-
r_{T2}	1.81	-
χ	0.995	-
η_i	0.41	-

The required compressor power was calculated from the following formulations:

$$\eta_C = \frac{h_5 - h_{6s}}{h_5 - h_6} \tag{11}$$

$$N_{i,C} = \dot{m}_{T1} \cdot (h_6 - h_5) \tag{12}$$

To calculate the thermodynamic parameters at the ejector outlet, the energy balance presented below was utilised:

$$\dot{m}_{T1} \cdot h_7 + \dot{m}_{T2} \cdot h_3 = (\dot{m}_{T1} + \dot{m}_{T2}) \cdot h_8 \tag{13}$$

The high temperature recuperator was modelled with the following set of equations:

$$\Delta T = T_2 - T_7 \tag{14}$$

$$\dot{m}_{T1} \cdot (h_2 - h_4) \cdot (1 - \epsilon_{HX}) = \dot{m}_{T1} \cdot (h_7 - h_6) \tag{15}$$

To take into account the heat losses from the heat exchanger to the environment the heat loss factor (ϵ_{HX}) was include in Eq. 15. Such approach is common in recent literature, i.e. [44, 45]. Finally, the thermal efficiency of the cycle is defined as:

$$\eta_i = \frac{N_{i,T1} + N_{i,T2} - N_{i,C}}{\dot{Q}_{heat}} \tag{16}$$

The parameters presented above were used to calculate the thermal properties of the CO_2 at the ejector inlets and outlet. To achieve the thermal efficiency of the cycle reported in [12], the desired mass entrainment ratio should be equal to 0.995.

4. Results and discussion

The on-design conditions for the ejector, considered for the system, were calculated to guarantee the thermal efficiency of the optimised cycle presented in [12]. The ejector operating regime defined by the system modelling is given in Tab. 2. The desired mass entrainment ratio for the operating regime

This is the accepted version of an article published in Energy.
DOI: 10.1016/j.energy.2018.09.030

Table 2: Ejector on-design operating conditions

Motive nozzle		**Suction nozzle**		**Outlet**
p, bar	t, °C	p, bar	t, °C	p, bar
250.00	304.4	127.10	569.10	230.00

presented in this table is equal to 0.995 to guarantee the required thermal efficiency of the system. Moreover, the system analysis results show that the required pressure lift in the ejector should be 103 bar. Therefore, the ejector applied in this sCO_2 cycle must fulfil both of these requirements.

All the operating conditions for the discussed ejector are distributed above the critical point. Therefore, the ejector presented in this study is considered as the single-phase unit. Nevertheless, the motive nozzle operating conditions for the ejectors developed for transcritical CO_2 refrigeration systems for hot climates usually are higher than at the carbon dioxide critical point. Therefore, the motive nozzle shape and the initial mixing section shape was designed using the procedures developed for such ejectors [35, 29]. In particular, first the motive nozzle throat diameter was designed according to the procedures presented in [35]. Next,the ratio between the mixing cross-section area to the motive nozzle cross-section area was defined similar to that presented in [35] or in [24]. The mentioned geometrical parameter was used to define the mixing section diameter, mixer length, and pre-mixing chamber length. According to the literature and the authors' experience, the diffuser diverging angle should be in the range between 3° and 5° for the highest efficiency. It is also evident that,the diffuser outlet has the minor effect on the ejector performance. Hence, that parameter was adapted from [41]. Moreover, the diffuser outlet diameter was a fixed parameter in the multi-parameter modifications of the initial shape of the device. Consequently, the length of this section is defined by the mixer diameter, the diffuser diverging angle and the diffuser outlet diameter. Similarly, the initial suction nozzle design was similar to that used in the previous work completed by this group [35]. Considering that the motive nozzle dimensions are crucial for the motive nozzle mass flow rate, the parameters describing that part of the device are listed in Tab. 3.

Table 3: Initial shape of the motive nozzle

Dimension	**Value**
Motive nozzle inlet diameter (D_{mn1}), mm	8.00
Motive nozzle throat diameter (D_{mn2}), mm	1.35
Motive nozzle outlet diameter (D_{mn3}), mm	1.45
Motive nozzle inner converging angle (γ_1), °	15.00
Motive nozzle diverging angle (γ_2), °	4.00
Motive nozzle tip diameter (D_{tip}), mm	2.00

Unfortunately, the performance of the initial ejector shape was not satisfying. The χ for the initial design was equal to 0. Consequently, the desired thermal efficiency of the cycle was impossible to achieve within the initial ejector design. Analysing the specific enthalpy and density field, as presented in Fig. 6, it can be seen that the expanding primary stream fills almost whole volume of the mixing section. Moreover, it was noticed that the velocity of the fluid did not decreased notably along the mixing section. Consequently, the desired mixing process of the primary and secondary stream was not fully developed. On the other hand, an increase in the mixing section diameter does not result in a higher χ for such high-pressure lift. That tendencies can be also noticed in Fig. 17 or in previous works of the

This is the accepted version of an article published in Energy.
DOI: 10.1016/j.energy.2018.09.030

authors, i.e. [27]. Therefore, to define the maximum mass entrainment ratio that can be achieve for the initial ejector design and the on-design motive and suction nozzle operating conditions the relationship between the pressure lift and recorded χ was investigated.

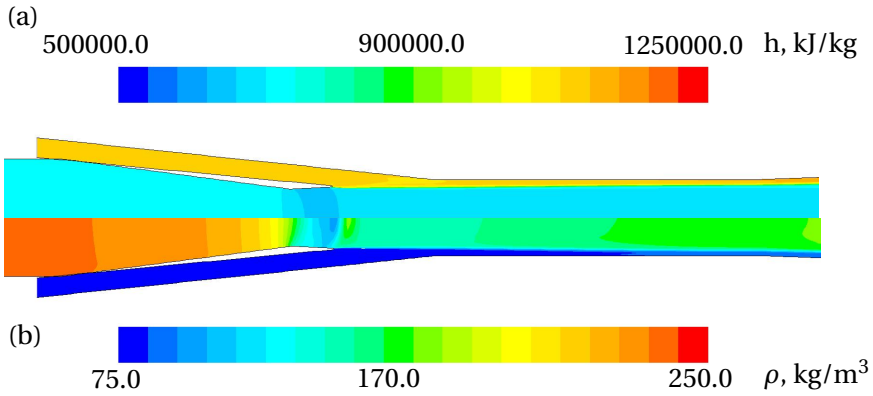

Figure 6: Fields of the specific enthalpy (a) and density (b) inside the mixing section of the ejector

The pressure lift for the ejector was modified by varying the ejector outlet/heater pressure. The results of this analysis for the initial ejector shape are presented in Fig. 7 as green dots. The highest-pressure lift with the positive suction nozzle mass flow rate was obtained at approximately 60 bar. Whilst, the maximum mass entrainment ratio was achieved for pressure lifts lower than 30 bar. The ejector performance was significantly lower than the required value to guarantee the system efficiency stated in [12]. Therefore, the initial shape of the ejector was modified to increase the mass entrainment ratio to 60 bar of pressure lift. For such pressure, the lift to mass entrainment ratio was equal to 0.087. The modification of the initial ejector shape focused mostly on the adaptation of the mixing section and the diverging part of the motive nozzle. Due to the ejector shape adaptation, χ substantially increased. The mass entrainment ratio for the modified ejector shape for various pressure lift is presented Fig. 7 as blue squares. Comparing the obtained results for the initial and the adapted ejector design, the new ejector shape offers a higher-pressure lift giving a higher mass entrainment ratio for a pressure lift of 60 bar. In contrast, the maximum χ possible with this ejector design was equal to 0.22. The maximum χ recorded for the pressure lift equals 28 bar and is 30% lower, when compared to the maximum χ noted for the base design. Moreover, the secondary stream was also significantly improved for the highest-pressure lift obtained within the ejector, mainly at 60 bar. In this case, the performance of the adapted ejector has improved by ~33%.

A comparison of the baseline ejector shape and the modified shape is presented in Tab. 4. The dimensions of the modified ejector presented in Tab 4 are defined as ratio of the initial dimension of the eject to modified dimension of the ejector, as it is following equation:

$$y = \frac{i_{modified}}{i_{initial}} \tag{17}$$

Each dimension describing the shape of the initial design was assumed to be equal to 1. Additionally, the influence of each modified parameter on χ is presented in Fig. 8. As shown in Fig. 8, the mixing section shape is crucial for the ejector performance. This result shows good agreement with previously published work on two-phase and single-phase ejectors [27, 41]. As expected, the mixer diameter is the most significant parameter that affects the pressure lift and mass entrainment ratio of the ejector. A

This is the accepted version of an article published in Energy.
DOI: 10.1016/j.energy.2018.09.030

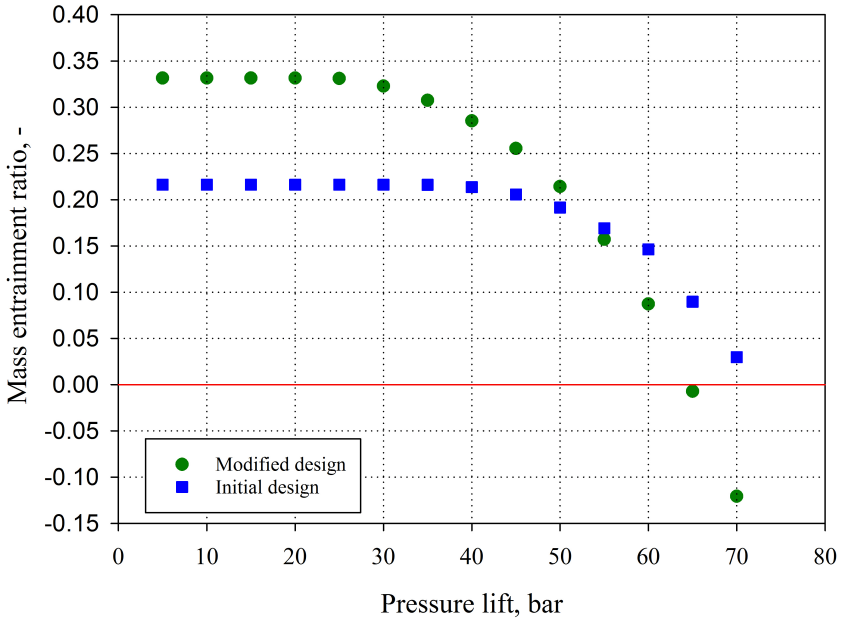

Figure 7: Relationship between the mass entrainment ratio and the pressure lift for the initial ejector design

reduction of the ejector diameter by 8% increased the mass entrainment ratio from 0.08 to 0.15. The modification of the motive nozzle outlet diameter also resulted in a slight increase in the ejector performance. However, it was significantly lower when compared to the mixer modifications.

The results of the motive nozzle diverging angle modifications are presented in Fig. 8, the variation of this parameter affects the χ notably. The improvement of the mass entrainment ratio within the modifications of the motive nozzle diverging angle is limited. Under considered conditions, the maxi-

Table 4: The ratio between initial and modified ejector design parameters

Dimension	***y***
Motive nozzle inlet diameter (D_{mn1})	1.00
Motive nozzle throat diameter (D_{mn2})	1.00
Motive nozzle outlet diameter (D_{mn3})	1.00
Motive nozzle inner converging angle (γ_1)	1.00
Motive nozzle diverging angle (γ_2)	1.50
Motive nozzle outer converging angle (γ_3)	1.00
Motive nozzle tip diameter (D_{tip})	0.75
Pre-mixing chamber length (L_{mch})	0.89
Mixer diameter (D_{mix})	0.92
Mixer length (L_{mix})	1.00
Suction nozzle converging angle (γ_{SN})	1.00
Diffuser outlet diameter (D_{diff})	1.00
Diffuser diverging angle (γ_{DIF})	1.00

This is the accepted version of an article published in Energy.
DOI: 10.1016/j.energy.2018.09.030

mum mass entrainment ratio is noted for a diverging angle adaptation which is equal to 0.1. This is still significantly lower than that required for efficient system operation.

Similar trends are noted for variations of the mixer length. The effects of the modification on the ejector performance is almost negligible giving minor changes in the ejector performance, within the premixing chamber length. Nevertheless, the variation of the ejector χ with a change in premixing chamber length is relatively small.

A decrease in the ejector pressure lift, directly results in the decrease of the heater pressure and whole system performance. Therefore, the considered sCO_2 system was modelled again to maximise the thermal efficiency for a fixed ejector pressure lift. Consequently, the ejector on-design conditions were changed. The list of the optimised system parameters, as well as a new set of the operating conditions for fixed ejector pressure lifts is presented in Table 5. For this new system, the thermal efficiency was equal to approximately 35%, which is significantly lower than that presented in Tab. 1. Hence, the thermal efficiency of the reference sCO_2 Brayton system, without the ejector installed, was not achieved [12]. The set up discussed is given in Tab. 5, once again this requires a relatively high χ for desired thermal efficiency.

Table 5: System parameters and ejector operating conditions for a fixed ejector pressure lift

	Pressure lift	
	60 bar	30 bar
r_{T_1}	2.996	2.996
r_{T_2}	1.013	1.027
χ	1.00	1.00
η_i	0.35	0.35

The discrepancies between the results presented in this manuscript and the reports of Padilla *et al.* [12] and are due to the novel approach for the ejector modelling. The results of the relatively simple 1D mathematical models are used for the ejector simulation, strongly depend on numerous assumptions, such as: the assumed efficiencies of the specific ejector sections, especially for the mixing section which is usually difficult to accurately determine. The mixing section efficiency used in [12] was defined for the steam ejector [13, 15], with the assumption of constant pressure at the inlet and outlet of the mixing section. Due to that definition and assumption of the mass entrainment ratio, the efficiency of the mixing section can be easily over estimated. These difficulties and the importance of the mixing section performance, as well as the efficiency predictions were previously discussed by the authors in [27]. The authors of that report show that the calculated ejector efficiency with various definitions can vary considerably. Moreover, the same authors, as well as the authors of [41], reported that the mixing section of the ejector section is responsible for most of the relative entropy increase and entropy generation.

5. Conclusions

The possibility of an ejector design suitable for the supercritical CO_2 Brayton cycle has been investigated. The ejector equipped sCO_2 system proposed by Padilla *et al.* [12] was considered as a reference layout. All the assumptions and input parameters proposed for the system and the ejector modelling were similar to that used in previous work discussed in [12]. The goal of the ejector design procedure was to achieve a mass entrainment ratio for the fixed pressure lift to guarantee the thermal efficiency of the system previously reported in [12].

This is the accepted version of an article published in Energy.
DOI: 10.1016/j.energy.2018.09.030

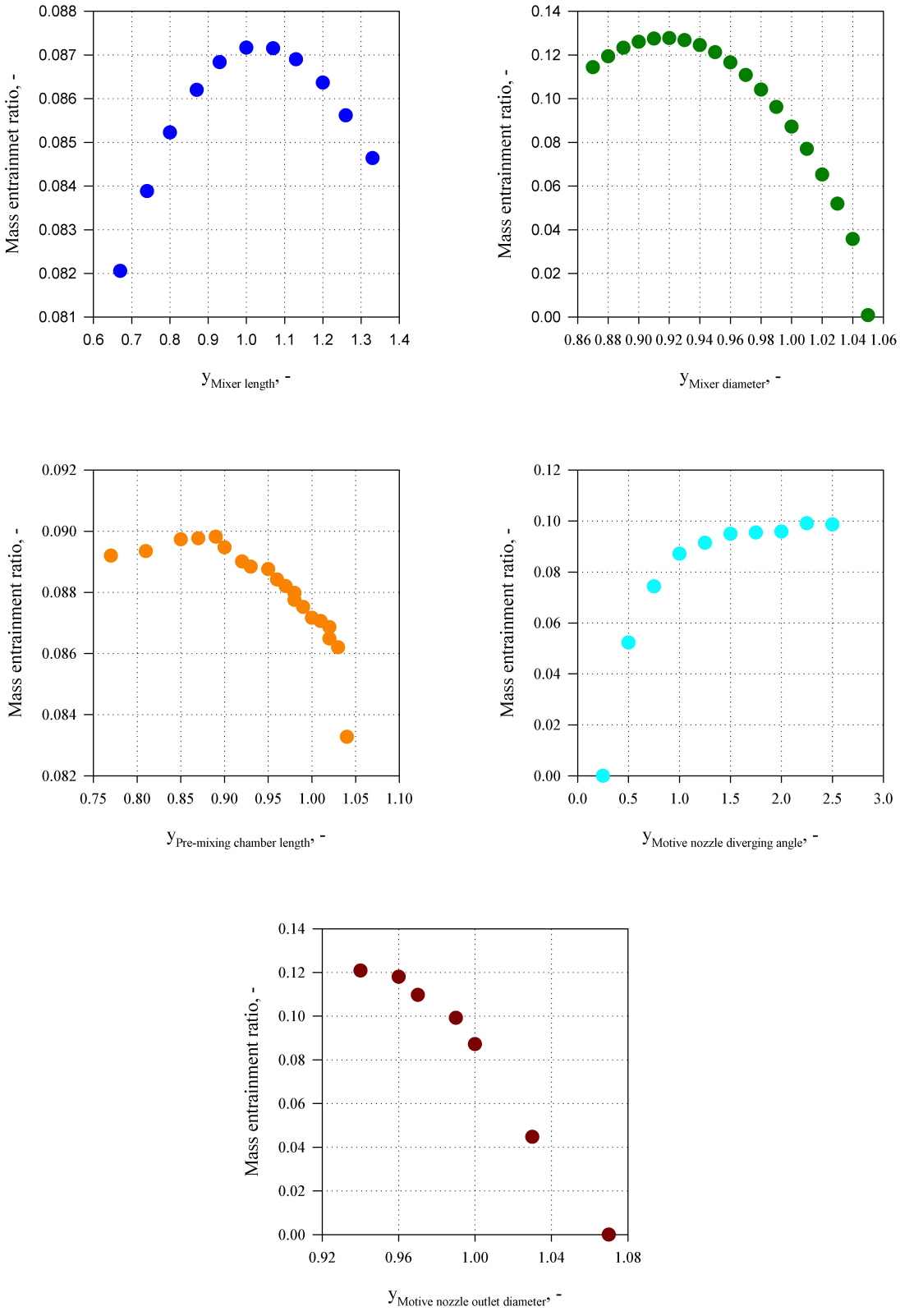

Figure 8: Influence of the ejector shape on its performance

This is the accepted version of an article published in Energy.
DOI: 10.1016/j.energy.2018.09.030

The obtained results showed that the ejector shape that meets the requirements presented in [12] was impossible to design. The performed investigation also showed that the maximum ejector χ for the defined motive nozzle operating conditions was reached for pressure lift equal to approximately 30 bar only, while the required pressure lift was 103 bar. Moreover, it was demonstrated in this paper that the incorrect definitions of the efficiency of each ejector section resulted in a significant overestimation of the ejector performance. Consequently, it was shown that the ejector-aided system analysis based on the relatively simple mathematical model of the ejector based on the arbitrary assumed partial efficiency can be misleading. In particular, the proper definition of the ejector mixing section efficiency is essential for the correct modelling of the ejector and the whole system.

The considered ejector for the analysed system was designed with an effective computational tool, *ejectorPL*, that was previously used for CO_2 ejector design in refrigeration systems. The initial ejector design was proposed and then the performance was investigated by employing *ejectorPL*. The preliminary ejector design was then modified to increase the performance of that device and sCO_2 system. The required mass entrainment ratio that will result the thermal efficiency of the reference system was not achieved. This was caused by the extreme pressure lift required. Therefore, the influence of the pressure lift on the mass entrainment ratio was analysed to define the maximum lift pressure for which the suction nozzle mass flow rate was positive. The highest-pressure lift obtained with the mentioned assumption was equal to 60 bar, with a corresponding mass entrainment ratio equal to 0.08.

The initial ejector design was modified to increase the χ for the 60 bar pressure lift conditions. The influence of such parameters as mixer diameter, premixing chamber length, mixer length, motive nozzle outlet diameter, and the motive nozzle diverging on the ejector performance was analysed. The collected results showed that, similarly to the two-phase ejectors used in refrigeration systems, the mixing section shape is crucial for the ejector performance. Even relatively small modifications of the mixer diameter notably affect the mass entrainment of the ejector. Because of the ejector shape modification, the χ significantly increased. In the case of 60 bar pressure lift, the mass entrainment ratio increases by 33% when compared to the initial design.

The thermal efficiency of the analysed system was assessed for a pressure lift equal to 30 bar and 60 bar. For this assumption, the system parameters were optimised to maximise η_i. Nevertheless, the thermal efficiency of the system by 35% for both the pressure lifts was significantly lower than for the reference system. Therefore, as with the authors of [12], the concept of the ejector implementation into the sCO_2 seems to be promising. Finally, the ejector that would guarantee an extreme pressure lift required by that system and simultaneously guarantee the mass entrainment ratio equal to almost 1 may be impossible to design.

Acknowledgments

The work of MH was partially supported by the SUT through project No. BKM-566/RIE6/2017. The work of MP was also partially supported by the Rector's research grant provided by SUT 08/060/RGJ17/0108.

References

[1] European Parliament and Council of the European Union, Regulation (EU) no 517/2014 of the european parliament and of the council of 16 april 2014 on fluorinated greenhouse gases and repealing regulation (EC) no 842/2006 text with EEA relevance.

[2] A. Mota-Babiloni, J. Navarro-Esbri, A. Barragan-Cervera, F. Moles, B. Peris, Analysis based on EU regulation no 517/2014 of new HFC/HFO mixtures as alternatives of high GWP refrigerants in refrigeration and HVAC systems, International Journal of Refrigeration 52 (2015) 21 – 31.

This is the accepted version of an article published in Energy.
DOI: 10.1016/j.energy.2018.09.030

[3] M.-H. Kim, J. Pettersen, C. W. Bullard, Fundamental process and system design issues in co_2 vapor compression systems, Progress in Energy and Combustion Science 30 (2004) 119 – 174.
[4] A. Pearson, Carbon dioxide - new uses for an old refrigerant, International Journal of Refrigeration 28 (2005) 1140 – 1148.
[5] G. Lorentzen, Revival of carbon dioxide as a refrigerant, International Journal of Refrigeration 17 (1994) 292 – 301.
[6] A. Mota-Babiloni, J. Navarro-Esbri, A. Barragan-Cervera, F. Moles, B. Peris, G. Verdu, Commercial refrigeration - an overview of current status, International Journal of Refrigeration 57 (2015) 186 – 196.
[7] A. Hafner, K. Banasiak, R744 ejector technology future perspectives, Journal of Physics: Conference Series 745 (2016) 032157.
[8] Y. Kim, C. Kim, D. Favrat, Transcritical or supercritical CO_2 cycles using both low- and high-temperature heat sources, Energy 43 (1) (2012) 402 – 415, 2nd International Meeting on Cleaner Combustion (CM0901-Detailed Chemical Models for Cleaner Combustion).
[9] Y. Ahn, S. J. Bae, M. Kim, S. K. Cho, S. Baik, J. I. Lee, J. E. Cha, Review of supercritical CO_2 power cycle technology and current status of research and development, Nuclear Engineering and Technology 47 (6) (2015) 647 – 661.
[10] F. A. Al-Sulaiman, M. Atif, Performance comparison of different supercritical carbon dioxide brayton cycles integrated with a solar power tower, Energy 82 (2015) 61 – 71.
[11] M. T. Luu, D. Milani, R. McNaughton, A. Abbas, Analysis for flexible operation of supercritical CO_2 brayton cycle integrated with solar thermal systems, Energy 124 (2017) 752 – 771.
[12] R. V. Padilla, Y. C. S. Too, R. Benito, R. McNaughton, W. Stein, Thermodynamic feasibility of alternative supercritical CO_2 brayton cycles integrated with an ejector, Applied Energy 169 (2016) 49 – 62.
[13] I. Eames, S. Aphornratana, H. Haider, A theoretical and experimental study of a small-scale steam jet refrigerator, International Journal of Refrigeration 18 (6) (1995) 378 – 386.
[14] N. H. Aly, A. Karameldin, M. Shamloul, Modelling and simulation of steam jet ejectors, Desalination 123 (1) (1999) 1 – 8.
[15] H. El-Dessouky, H. Ettouney, I. Alatiqi, G. Al-Nuwaibit, Evaluation of steam jet ejectors, Chemical Engineering and Processing: Process Intensification 41 (6) (2002) 551 – 561.
[16] A. A. Kornhauser, The use of an ejector as a refrigerant expander, 1990.
[17] F. Liu, E. A. Groll, D. Li, Investigation on performance of variable geometry ejectors for CO_2 refrigeration cycles, Energy 45 (1) (2012) 829 – 839, the 24th International Conference on Efficiency, Cost, Optimization, Simulation and Environmental Impact of Energy, ECOS 2011.
[18] K. Banasiak, A. Hafner, 1D computational model of a two-phase R744 ejector for expansion work recovery, International Journal of Thermal Sciences 50 (11) (2011) 2235 – 2247.
[19] K. Banasiak, A. Hafner, Mathematical modelling of supersonic two-phase R744 flows through converging-diverging nozzles: The effects of phase transition models, Applied Thermal Engineering 51 (1) (2013) 635 – 643.
[20] J. Smolka, Z. Bulinski, A. Fic, A. J. Nowak, K. Banasiak, A. Hafner, A computational model of a transcritical R744 ejector based on a homogeneous real fluid approach, Applied Mathematical Modelling 37 (3) (2013) 1208 – 1224.
[21] M. Palacz, J. Smolka, A. Fic, Z. Bulinski, A. J. Nowak, K. Banasiak, A. Hafner, Application range of the hem approach for CO_2 expansion inside two-phase ejectors for supermarket refrigeration systems, International Journal of Refrigeration 59 (2015) 251 – 258.
[22] C. Lucas, H. Rusche, A. Schroeder, J. Koehler, Numerical investigation of a two-phase CO_2 ejector, International Journal of Refrigeration 43 (2014) 154 – 166.
[23] M. Palacz, M. Haida, J. Smolka, A. J. Nowak, K. Banasiak, A. Hafner, HEM and HRM accuracy comparison for the simulation of co2 expansion in two-phase ejectors for supermarket refrigeration systems, Applied Thermal Engineering 115 (2017) 160 – 169.
[24] M. Haida, J. Smolka, A. Hafner, M. Palacz, K. Banasiak, A. J. Nowak, Modified homogeneous relaxation model for the R744 trans-critical flow in a two-phase ejector, International Journal of Refrigeration 85 (2018) 314 – 333.
[25] G. Besagni, R. Mereu, P. Chiesa, F. Inzoli, An integrated lumped parameter-CFD approach for off-design ejector performance evaluation, Energy Conversion and Management 105 (2015) 697 – 715.
[26] M. Haida, J. Smolka, A. Hafner, Z. Ostrowski, M. Palacz, K. B. Madsen, S. FÃűrsterling, A. J. Nowak, K. Banasiak, Performance mapping of the R744 ejectors for refrigeration and air conditioning supermarket application: A hybrid reduced-order model, Energy 153 (2018) 933 – 948.
[27] K. Banasiak, M. Palacz, A. Hafner, Z. Bulinski, J. Smolka, A. J. Nowak, A. Fic, A CFD-based investigation of the energy performance of two-phase R744 ejectors to recover the expansion work in refrigeration systems: Anirreversibility analysis, International Journal of Refrigeration 40 (2014) 328 – 337.
[28] J. Bodys, M. Palacz, M. Haida, J. Smolka, A. J. Nowak, K. Banasiak, A. Hafner, Full-scale multi-ejector module for a carbon dioxide supermarket refrigeration system: Numerical study of performance evaluation, Energy Conversion and Management 138 (2017) 312 – 326.
[29] M. Palacz, J. Smolka, A. J. Nowak, K. Banasiak, A. Hafner, Shape optimisation of a two-phase ejector for CO_2 refrigeration

This is the accepted version of an article published in Energy.
DOI: 10.1016/j.energy.2018.09.030

systems, International Journal of Refrigeration 74 (2017) 212 – 223.
[30] B. Stankovic, Brayton or Brayton-Rankine Combined Cycle With Hot-Gas Recirculation and Inverse Mixing Ejector, 2002.
[31] P. Garg, P. Kumar, K. Srinivasan, Supercritical carbon dioxide brayton cycle for concentrated solar power, The Journal of Supercritical Fluids 76 (2013) 54 – 60.
[32] D. Milani, M. T. Luu, R. McNaughton, A. Abbas, A comparative study of solar heliostat assisted supercritical CO_2 recompression brayton cycles: Dynamic modelling and control strategies, The Journal of Supercritical Fluids 120 (2017) 113 – 124.
[33] F. Crespi, G. Gavagnin, D. Sanchez, G. S. Martinez, Supercritical carbon dioxide cycles for power generation: A review, Applied Energy 195 (2017) 152 – 183.
[34] R. Singh, M. P. Kearney, C. Manzie, Extremum-seeking control of a supercritical carbon-dioxide closed brayton cycle in a direct-heated solar thermal power plant, Energy 60 (2013) 380 – 387.
[35] K. Banasiak, A. Hafner, E. E. Kriezi, K. B. Madsen, M. Birkelund, K. Fredslund, R. Olsson, Development and performance mapping of a multi-ejector expansion work recovery pack for R744 vapour compression units, International Journal of Refrigeration 57 (2015) 265 – 276.
[36] S. Croquer, S. Poncet, Z. Aidoun, Turbulence modeling of a single-phase R134a supersonic ejector. part 1: Numerical benchmark, International Journal of Refrigeration 61 (2016) 140 – 152.
[37] J. Anderson, Computational Fluid Dynamics, Computational Fluid Dynamics: The Basics with Applications, McGraw-Hill Education, 1995.
[38] T. Chung, Computational Fluid Dynamics, Cambridge University Press, 2002.
[39] E. W. Lemmon, M. L. Huber, M. O. McLinden, NIST Standard Reference Database 23: Reference Fluid Thermodynamic and Transport Properties - REFPROP, National Institute of Standards and Technology, Standard Reference Data Program, Gaithersburg, 9th Edition (2010).
[40] M. Haida, J. Smolka, A. Hafner, Z. Ostrowski, M. Palacz, A. J. Nowak, K. Banasiak, System model derivation of the CO_2 two-phase ejector based on the CFD-based reduced-order model, Energy 144 (2018) 941 – 956.
[41] J. Sierra-Pallares, J. G. del Valle, P. G. Carrascal, F. C. Ruiz, A computational study about the types of entropy generation in three different r134a ejector mixing chambers, International Journal of Refrigeration 63 (2016) 199 – 213.
[42] M. Palacz, J. Smolka, W. Kus, A. Fic, Z. Bulinski, A. J. Nowak, K. Banasiak, A. Hafner, CFD-based shape optimisation of a CO_2 two-phase ejector mixing section, Applied Thermal Engineering 95 (2016) 62 – 69.
[43] M. Reyes-Belmonte, A. Sebastian, M. Romero, J. Gonzalez-Aguilar, Optimization of a recompression supercritical carbon dioxide cycle for an innovative central receiver solar power plant, Energy 112 (2016) 17 – 27.
[44] V. Ganapathy, Simplify heat recovery steam generator evaluation, Hydrocarbon Processing;(USA) 69 (3).
[45] M. Plis, H. Rusinowski, Adaptive simulation model of a double-pressure heat recovery steam generator for current optimization in control systems, IEEE Transactions on Industry Applications 53 (1) (2017) 530–537.

This is the accepted version of an article published in Energy.
DOI: 10.1016/j.energy.2018.09.030